Design and Fabrication of Wideband Dual-Polarized Dipole Array for 5G Wireless Systems

SAJJAD HUSSAIN, (Student Member, IEEE), SHI-WEI QU, (Senior Member, IEEE), WEN-LIANG ZHOU, PENG ZHANG, AND SHIWEN YANG, (Fellow, IEEE)

School of Electronic Science and Engineering, University of Electronic Science and Technology of China (UESTC), Chengdu 611731, China

Corresponding author: Shi-Wei Qu (shiweiqu@uestc.edu.cn)

ABSTRACT This paper presents simulation and measurement results of a wideband planar phased array for 5G. The desired wideband operation is achieved using a tightly coupled dipole array (TCDA). The proposed array consists of tightly coupled dipole units in dual-polarized configuration, and two thin parasitic layers separated apart by air gap for wide-angle impedance matching (WAIM). The top matching layer is loaded with a metasurface composed of sub-wavelength split-ring resonators (SRRs) to improve the scanning performance of array. The infinite array achieved a bandwidth from 23.5 to 29.5 GHz, with voltage standing wave ratio (VSWR) < 3 for scan up to $\pm 60°$ in E, H and D-plane. The array has a height of only $0.144\lambda_l$, and it exhibits high gains, high efficiency $> 71\%$ (largest scan angle) and good cross-polarization. The simulations are validated by fabrication and measurement of an array prototype, which indicates agreement to simulated values. The proposed dual-polarized antenna array can be deployed in the future beam scanning applications for 5G.

INDEX TERMS 5G, millimeter-wave, phased arrays, planar arrays, metasurface.

I. INTRODUCTION

In less than a decade, 5G has transformed from a merely a distant concept to a reality with wireless access and services begin to roll out across the globe. No doubt, 5G is not an evaluation but a big revolution unlike predecessor generations. Thus in order to achieve its full potential requires end-to-end network transformations.

5G technology promise extensive improvement in capacity to accommodate ever-increasing data demands. Millimeter-Wave bands are widely considered as prospective candidate for 5G, due to the large bandwidths that can be exploited to improve the channel capacity, along with much-desired high data rates for users [1].

International Telecommunication Union (ITU) has proposed several millimeter–wave bands (above 24 GHz to 100 GHz) for fifth generation (5G) technology [2]. 26 GHz (24.25 to 27.50 GHz) and 28 GHz (26.50 to 29.50 GHz) bands are the two most promising bands for preliminary

The associate editor coordinating the review of this manuscript and approving it for publication was Davide Ramaccia.

5G commercial deployment. Although, increasing the frequency, will result in higher path loss as evident from Friis formula [3]. One possible solution is to enlarge the antenna aperture to achieve large transmission distances. Even though this can improve the antenna gain, the demerit is narrow beam-width with limited coverage area. Therefore, in order to achieve both high gain and wide coverage for possible 5G mobile terminals, the use of phased array is a promising solution.

Planar phased arrays with high-gain performance and agile beam switching are a key ingredient to unlock the true potential of 5G technologies, to ensure coverage and better capacity at commercially allocated millimeter-wave spectrum. Thus, many companies and research groups are rushing to design fixed wireless access and radio front/backhaul equipment for 5G technology.

Historically, mutual coupling amongst the elements was considered as a complication in the design of conventional phased arrays. However, this is not the case, for tightly coupled arrays (TCAs). These arrays exhibit characteristics like wide band, wide-scan, low profile and low cross polarization

levels, these features are in demand for future wireless radio frontends. TCAs utilize capacitive coupling between electrically small elements to support low-frequency operation across a relatively large sub-array aperture with multiple elements, and consequently the current distribution can be equivalent to a sheet with uniform current as theoretically proposed by Wheeler [4]. Meanwhile, B. A. Munk gave an explanation to the bandwidth enhancement from the input impedance point of view, i.e., due to the cancellation of the inductance from the ground by the capacitance of the tightly coupled elements. This was implemented on capacitively coupled dipoles with dielectric layers above the ground plane for the first time in 2003 [5]. Many TCDA based phased arrays has been designed in recent years mainly for sub-6 GHz [6]–[8], X-band [9]–[11] and Ku-band [11]–[13]. However, very few millimeter wave bands designs are reported, for commercial applications. Although, TCAs are in military use for many years with very wideband capabilities, however, due to the release of millimeter-wave frequencies for 5G these arrays are now actively considered for commercial deployment. The commercial demands are different from military. An ultrawideband (UWB) phased array, capable of covering 5G bands in millimeter wave spectrum with VSWR < 3 for ±45° scanning in E and H-plane [14]. Another millimeter wave differential phased array [15] with polarization diversity across 5G bands is excited by twin line differential feed. Most of these designs are single polarized with maximum scanning range ±45° (see section III for comparison). The main contribution of this work is to design and verify the phased array with below mentioned goals.

1) An array with sufficient bandwidth to cover both 26 and 28 GHz bands. Since these are preliminary bands for 5G commercial deployment at millimeter-wave spectrum, with active VSWR < 3 over the scan range.
2) Scan up to ±60° in all planes.
3) Planar geometry with simple feeding structure.

The mentioned objectives are not reported in literature so far, particular to preliminary commercially attractive 5G bands to the author's knowledge. In this work a 12×12 array prototype is manufactured using the standard PCB technology, operating over 23.5 -29.5 GHz. The prototype array is achieving over 23% fractional bandwidth with active VSWR < 3 while scanning up to ±60°, in all planes. The measured performance is in good agreement with the simulation results, with array presenting good beam steering property in E, H and D-plane. The metasurface consists of SRRs is used for impedance matching, metasurfaces are more actively used in different antenna designs as it is used for linear-to-circular polarization conversion in [16]. The radiation and scattering performances are presented and discussed to verify the design.

The paper is organized as follows. Section II discusses the design method, working principle and simulated performance of unit cell. Fabrication details of array, comparison between simulation and measurement results are given in Section III and Section IV provides the conclusion of this work.
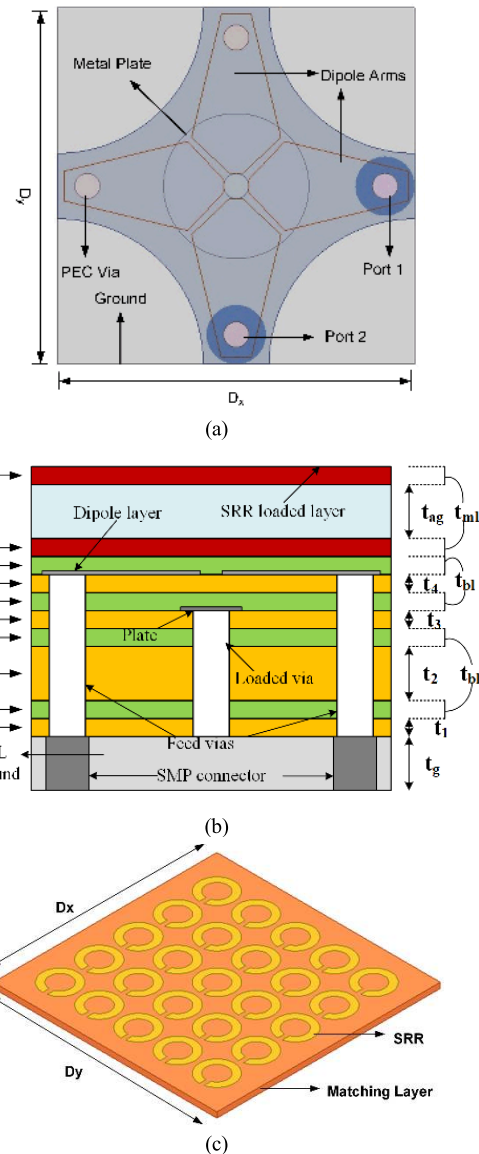
FIGURE 1. Geometry of TCDA unit element (a) Top view without matching layers (b) Side view (green indicates bonding layers) (c) SRR loaded matching layer (isometric view).

II. ANTENNA CONFIGURATION AND OPERATING PRINCIPLE

The detailed configuration of the proposed unit cell is shown in Fig. 1. The antenna element consists of dipoles, a circular plate, two WAIM layers, a pair of 50Ω SMP connector and a ground plane. The radiating layer consists of dipoles arranged in a dual-polarized frame with strong capacitive coupling amongst cross-polarized elements. The tightly coupled dipoles placed over the ground plane and matching layers altogether provide wideband operation and wide-scan performance. Capacitively coupled dipoles are implanted on dielectric material layers above the ground plane in orthogonal topology to achieve dual polarized aperture. Although, array elements, are placed in close proximity to the ground

plane ($0.15\lambda_h$), but still maintained good radiating efficiency because, the input impedance is well matched.

The dipoles are fed by perfect electric conductor (PEC) vias. The metallic plate is printed on dielectric beneath the dipole arms loaded with a shorting via. The upper wide-angle impedance matching layer loaded with split-ring resonators (SRRs) is used to improve scanning performance especially in H-plane.

The dipole arms are printed on substrate layers, bonded together using Rogers RO4450F bondply with $\varepsilon_r = 3.52$, $\tan\delta = 0.004$, with thickness of 0.101 mm. Rogers RT/duriod 5880 with $\varepsilon_r = 2.2$, $\tan\delta = 0.0009$ is used as aperture substrate. Two layers each 0.13 mm thick of Rogers RO3003 $\varepsilon_r = 3$, $\tan\delta = 0.0010$, apart by an air gap of 2 mm is placed above dipoles acts as Wide Angle Impedance Matching (WAIM) layer. 7 mm thick, aluminum is acting as ground, appropriate thickness is chosen to accommodate fuzz button based SMP connector. The square unit cell has length 5.4 mm a little more than half of wavelength, at the highest frequency.

The unit element simulations are carried under periodic boundary condition using HFSS. The radiating layer consists of dipoles arranged in a dual-polarized frame with strong capacitive coupling amongst cross-polarized elements. The tightly coupled dipoles placed over the ground plane and matching layers altogether provide wideband operation and wide-scan performance.

Impedance matching is fundamental in order to achieve a wideband radiating aperture. Hence, careful selection and optimization of element type and coupling, spacing of ground plane, and parasitic matching layers resulted in almost constant impedance for our desired frequency band.
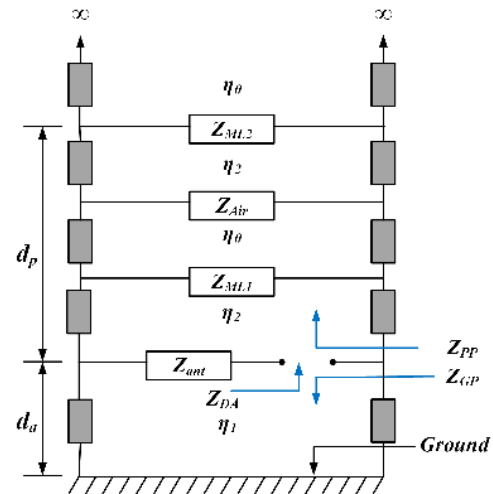
A. IMPEDANCE

The working principle of array is based on Munk current sheet array (CSA) concept [5]. The theoretical background of CSA is based on analyzing the impedance response of each component in the design to attain total impedance behavior of array. Suitable selection of antenna element type and coupling, spacing from ground plane, and matching layers results in almost constant impedance over wide range of frequencies although, the individual impedance values vary over frequency. The capacitive coupling among neighboring elements is utilized to overcome inductive loading from ground plane.

Some assumptions are made to apply CSA approach that includes the array is of infinite size, the elements are electrically short. Following the mentioned assumptions, the equivalent circuit of array of tightly coupled dipoles spaced above ground plane with two dielectric layer above the elements is shown in Fig. 2, which is an accurate equivalence of the impedance response of the array.

Impedance observed from array terminals combine in parallel, thus input impedance of dipole arms $Z_{ant} = Z_{GP} + Z_{PP}$. The impedance viewed from the array terminals towards

TABLE 1. Unit cell geometric parameters and dimensions.

| Thickness	Value (mm)	Dimensions	Value (mm)
$t_{1,3,4}$	0.127	r_{plate}	1.1
t_2	0.787	D_x, D_y	5.4
t_{bl}	0.101	r_{via}	0.2
t_{ml}	0.13	ε_{r1}	2.2
t_{ag}	2	ε_{r2}	3.52
t_g	7	ε_{r3}	3.0

FIGURE 2. Equivalent circuit of array.

the ground plane is Z_{GP} and is the impedance viewed from the array terminals towards free space through the WAIM layers is Z_{PP}. The impedances viewed from array terminals combined in parallel because these values are transformed along the suitable electrical distances to be coincident at array terminals.

Just assume for one polarization, E and H planes are aligned similar as x and y-axis respectively, thus TE and TM polarizations are in y and x directions, respectively. The lattice spacing between the metasurface elements is much smaller than the array itself therefore, and therefore metasurface can be considered as homogenized structure in *xy* plane. Similar assumption can be made for other polarization in dual polarization case. The impedance perceived by dipole arms is not the impedance of just metasurface itself but free space impedance behind the metasurface is shunted with it. Referring to [17] in TM polarization, a small reactive component is due to metasurface impedance. Thus, the impedance looking into the metasurface backed by free space is quite similar to free-space TM wave impedance. The TM polarization dominates in E-planes, and thus verifies and explains the outcome of metasurface minimum impact on E-plane scan, with a significant improvement in H-plane scan.
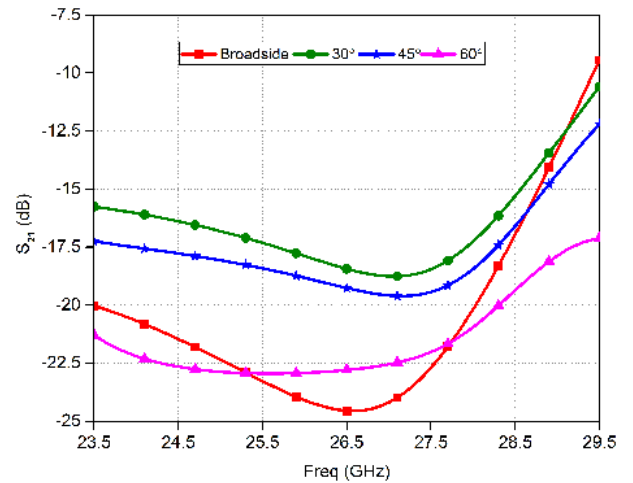
B. INFINITE ARRAY PERFORMANCE

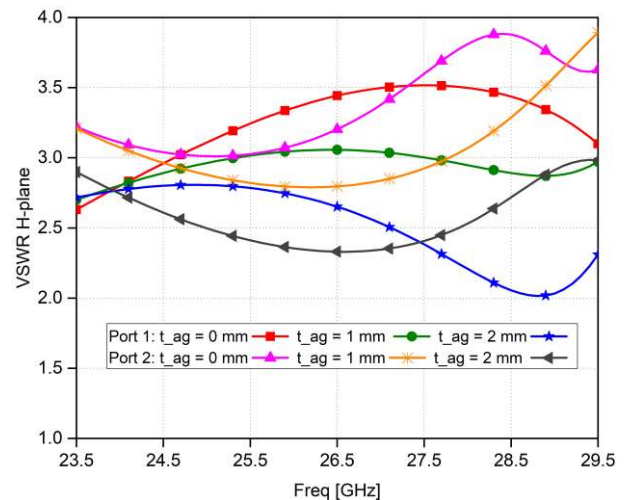Unit element impedance well matched to 50Ω input impedance leading to wideband operation. VSWR values for
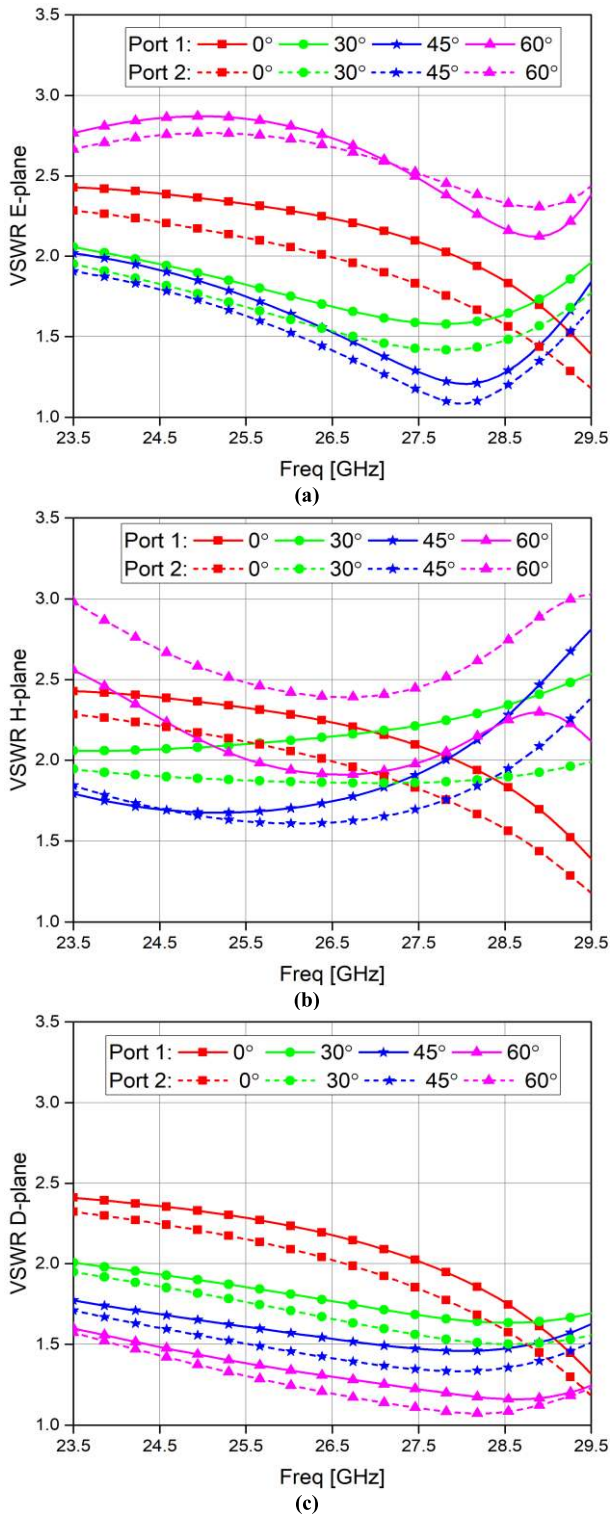
FIGURE 3. Simulated infinite array VSWR Port 1 and 2 (a) E-plane (b) H-plane (c) D-plane.

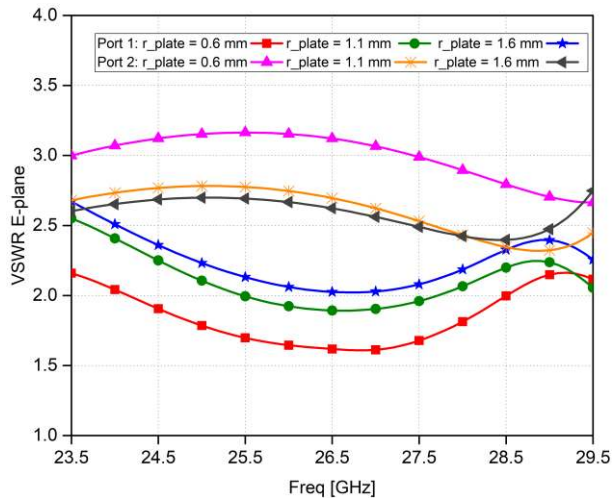**FIGURE 4.** Orthogonal port isolation vs. frequency for broadside and scans.

FIGURE 5. Air gap variations between matching layers, and its effect on 60° H-plane scan performance.

all planes, the array maintains 6 dB return-loss operating bandwidth from 23.5 to 29.5 GHz.

The array also exhibits high cross-polarization isolation. The port isolation remains below −10 dB for all scan cases across the band as depicted in Fig. 4. Thus, acceptable port isolation amongst the two ports made it possible, to simulate and measure the finite array under single polarization excitation.

C. ROLE OF MATCHING LAYERS

Use of dielectric WAIM is one way to increase the bandwidth of TCDA. These superstrates act as impedance matching sections in order to match the impedance of array with free-space impedance. In this design a metasurface loaded with a parasitic layer of sub-wavelength SRRs is used. A 5×5 sheet of SRR having lattice spacing $\Delta_{x,y} = 0.08\lambda_0$ is deployed (Fig. 1. c).

both ports of unit cell are shown in Fig. 3. It is observed that the VSWR remains < 2.5 across the almost entire band at broadside and scans up to ±45° for both planes. Furthermore, when scanning even up to ±60° for both polarizations in

FIGURE 6. Variations in the radius of via loaded metal plate and corresponding E-plane 60° scan.

FIGURE 7. Fabricated 12 × 12 array prototype, (a) top view, without matching layers, showing etched dipoles (b) bottom view of ground plane with 64-element excited using fuzz button based SMP connector.

The SRR response depends on a magnetic vector normal to the plane containing the split rings hence; metasurface is tuned to improve the scan range of array in H-plane, as already explained. Due to the appropriate distance $0.2\lambda_0$ above dipole arms and sub-wavelength size of SRRs (nearly $0.1\lambda_0$), H-plane scan up to ±60° is achieved.

Metasurface loaded matching layer over the dipole arms with suitable distance from dipoles is influential to achieve wide H-plane scan, as already explained. Simulated variations with different air gap variations for just ±60° scan for both ports are presented in Fig. 5. As evident, a 2 mm gap is appropriate to achieve 60° scan in for both polarizations.
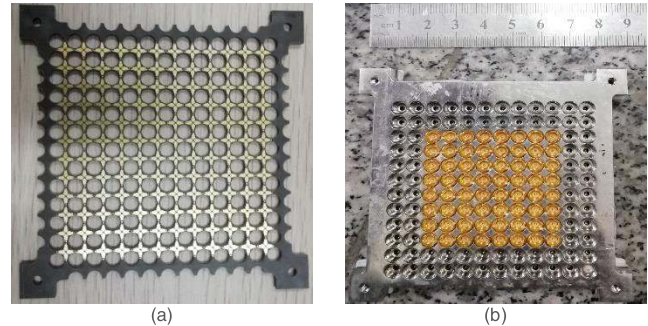
D. ROLE OF METAL PLATE

Array elements are closely spaced, separated by a small gap. The gap created capacitance between the neighboring elements and is useful in achieving wideband. Capacitance is further facilitated by introducing a circular plate. This metallic plate etched beneath the dipoles is loaded with via. This configuration is helpful to mitigate the common mode resonance at the broadside, without affecting the bandwidth at the lower end of the band. Moreover, this structure boosts inter-dipole capacitance and is useful to achieve wide scan E-plane performance.

After attempting several radii of the metal plate, a suitable size presented here is the best in terms of wide-scan performance. To elaborate the influence on beam scan of the wide-scan E-plane performance, some random variations are shown in Fig. 6 for 60° scan.

III. PROTOTYPE FABRICATION AND RESULTS

A 12 × 12 array is fabricated with Port 2 excitation with Port 1 as short circuit, to avoid too much simulation resources and time, since dual polarizations have already been verified for an 8 × 8 array [18]. As evident from unit element outcomes both polarizations are identical and orthogonal to each other

with acceptable orthogonal port isolation thus, validation of one validates the other. Tile architecture arrays is an industry trend, where different layers placed parallel to the face, integrated into a single multilayer structure with Tx/Rx modules loaded beneath. Same approach is used to feed the designed array.
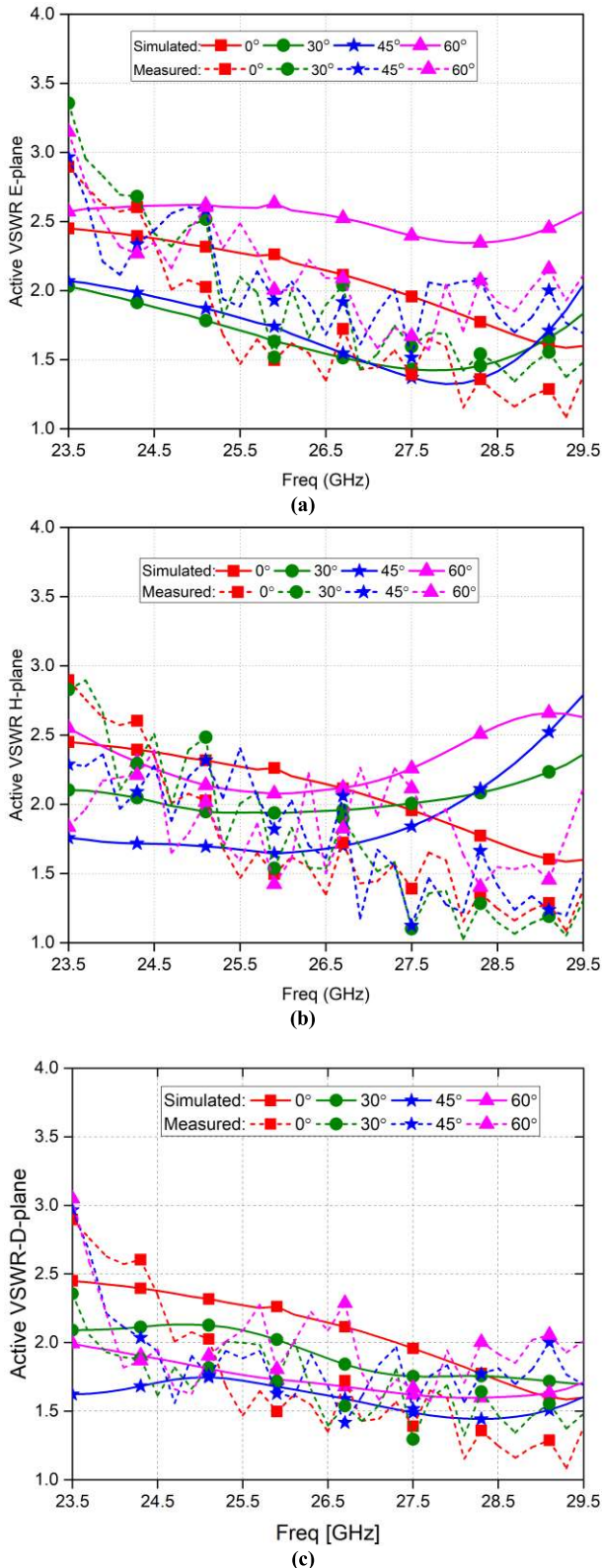
Prototype array is a low cost, multilayer PCB arrangement, as depicted in Fig. 7. The air gap is replaced by 2 mm thick Rohacell material with $\varepsilon_r = 1.09$ and $\tan\delta = 0.0015$. Four holes one at each corner is drilled through the array PCB dielectric layers, to fasten the PCB with ground to perform measurements. An aluminum ground, with special 0.02 mm tin coating, in order to bond with multilayer substrate with total thickness of 7 mm is placed under the substrate, to accommodate fuzz button based SMP connector. Spring like fuzz button connector is used for a solider less connection in order to excite the array. The overall dimensions of 12 × 12 array are $85.6 \times 85.6 \times 10.7$ mm^3.

The bandwidth of finite array is affected when array aperture is truncated. Finite array bandwidth not only depends on the aperture shape and size, but also on type of element. It is observed that the elements towards the array periphery when excited detune the active VSWR of center elements. To minimize the effect of finite array on performance, edge element termination technique is used. This is done by exciting elements around the center of array and not exciting the peripheral elements as shown in Fig. 7 (b).
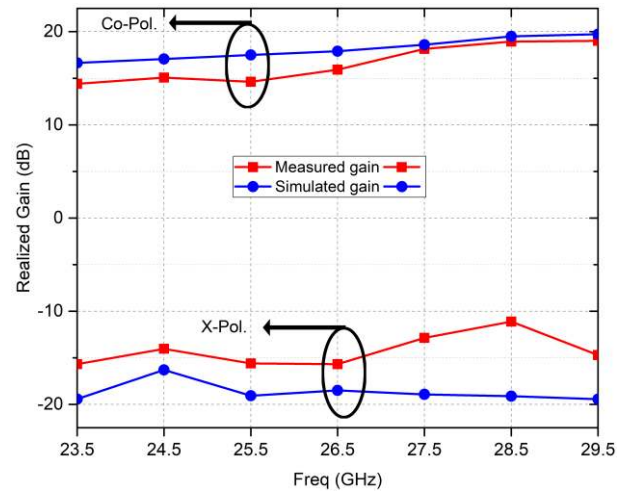
A. ACTIVE VSWR

In array scenario, all elements are excited together. Therefore, active VSWR that considers the effect mutual coupling is used to analyze. The active VSWR (50Ω) is measured at a central element of array to validate the scan performance. The reflection coefficient of selected port and the transmission coefficient between this port and all other ports are measured one by one using a vector network analyzer (N5244A). Later the active reflection coefficient of central element is calculated using summation formula given below.

$$Active\ S_m = \sum_{n=1}^{N} \frac{a_n}{a_m} S_{mn} \quad m = 1, 2, \dots, N \qquad (1)$$

FIGURE 9. Measured (Red) and simulated (Blue) broadside realized gain of 32 elements in array (16 for each polarization) versus frequency.

FIGURE 8. Simulated (solid line) and measured (dotted line) active VSWR for 8 × 8 excited elements (a) E-plane (b) H-plane (c) D-plane.

Here Active S_m symbolizes the reflection coefficient of central element. S_{mn} is the measured complex S-parameter between Ports m and n, a_m and a_n are the corresponding

complex excitations, and N is the count of elements. Eventually, the active VSWR of central element is $(1 + \text{Active } S_m)/(1 - \text{Active } S_m)$.
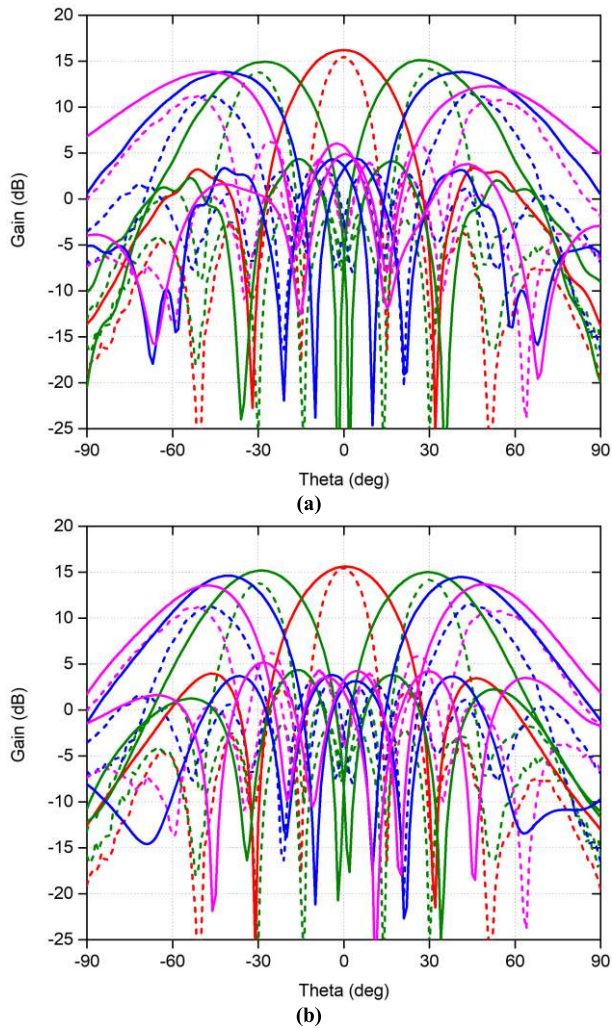
Both full wave simulation results and measurement outcomes agree reasonably well with each other, successfully demonstrate broad impedance bandwidth from 23.5 to 29.5 GHz out to ±60° scan in E, H and D-planes. The measured 8 x 8 array active VSWR results, which are compared with the simulated values of the array with same number of elements as shown in Fig. 8 (a, b, c). The measured values largely follow the same trends as the array simulations, however a slight upward shift of values is observed. The measured active VSWR remains < 3 across almost entire band except for a few lower frequencies for E-plane. Better active VSWR values are observed at the upper end of the band, during measurements.

The minor disagreement at the band edges is due to fabrication tolerance and the impact of high frequency connectors. Nonetheless, results show acceptable performance over the operational band. The array presents an effective and low-cost solution for beam scan implementation for 26 and 28 GHz 5G bands.

B. ARRAY POLARIZATION AND EFFICIENCY

The measured broadside realized gain for 32 elements (16 for each polarization) as a function of frequency is plotted in Fig. 9, corresponding simulated gain is given for comparison. The measured co-polarized gain is in good consistency with the simulations, with less than 2.2 dB variations, indicating high efficiency. The measured cross-polarization values hover around −15 dB. Good agreement is observed for co-polarized and cross-polarized gain values, verifying the finite array simulations.

The measurements of radiation pattern are obtained by unit excitation active element pattern (UEAEP) method [19]. Using this far field gain patterns of array elements are

FIGURE 10. Measured (dashed line) and simulated (solid line) scan patterns of array (32 elements) at 26.5 GHz for scan to 0° (Red), ±30° (Green), ±45° (Blue) and ±60° (Magenta) (a) E-plane (b) H-plane.

TABLE 2. Comparison with some recent designs.

Ref.	$D_x \times D_y$ᴬ	D_zᴬ	Max. scan angle E & H-plane	Polarization
[14]	0.49×0.49	0.39	± 45°	Single
[15]	0.47×0.47	0.38	± 60°	Single
[20]	0.44×0.44	0.37	± 60°	Dual
[21]	0.48×0.48	0.37	± 45°	Single
Our	0.53×0.53	0.37	± 60°	Dual

ᴬ in terms of λ_h

The efficiency of finite array is calculated using Eq. 2, for broadside and different scan angles. This presents the percentage of accepted power radiated. It accounts for loss in conductors and dielectrics, as well as the influence due to cross polarizations. Highest value of efficiency is observed at 29.5 GHz > 87% for broadside and lowest value is > 71% for scan to ±60° at 26.5 GHz.

$$\eta_{array} = \frac{Total\ radiated\ power}{Total\ excited\ power} \qquad (2)$$

In Table 2 , the proposed array is compared with the recent millimeter wave arrays publications in terms of maximum scan range and array profile. Although, the prototypes listed in the table 2 are nearly same profile and size, mostly only achieve maximum scan angle to ±45° under single polarized case. It is noted that this work achieved a wide scan range while having element size nearly equal to half of a wavelength at the highest frequency. Moreover, the proposed array has a wider scan range as well as thin superstrates and largest unit element size. These attributes along with same scan range in both planes for both polarizations make it a suitable choice for utilization at promising 26 and 28 GHz bands, which are actively considered for preliminary 5G commercial launch.

IV. CONCLUSION

The design, simulation and measurement results for a wideband dual-polarized tightly coupled phased array have been presented. The array is low-profile, wide-scan and has good cross-polarization and consistent radiation patterns. The top metasurface loaded parasitic layer is beneficial to achieve wide H-scan performance, while the circular metallic plate is handy to achieve wide scan in E-plane. The measured results show that the scanning range of the designed array with metasurface loaded matching layer is up to ±60° in E, H and D-planes at 26 GHz and 28 GHz 5G bands. Measurements confirm the feasibility of the antenna for 5G base station applications due to its compactness and wide scanning in three planes.

measured one after the other in the anechoic chamber, with other ports being terminated with 50Ω matched loads. The measured element gain patterns are then combined with equal amplitude weightings and corresponding progressive phase.

Fig. 10 (a, b) present the measured radiation patterns at central frequency (26.5 GHz) while scanning to broadside, ±30°, ±45°, and ±60° in E and H-plane, respectively. Since the pattern and maximum scan angles that are already verified for E and H-plane, therefore, the D-plane scanning is not shown here because it is an approximate average, of the principle planes scanning.

The arrays beams are well maintained with specific directivities as the array is scanned. It is evident that measured pattern outcomes are in agreement with simulated. The minor discrepancies are mainly due to surface waves that only exist in finite array and propagate along the array, because of reflections from the array edges.

REFERENCES

[1] J. G. Andrews, S. Buzzi, W. Choi, S. V. Hanly, A. Lozano, A. C. K. Soong, and J. C. Zhang, "What will 5G be?" *IEEE J. Sel. Areas Commun.*, vol. 32, no. 6, pp. 1065–1082, Jun. 2014.

[2] *Report of the CPM on Technical, Operational and Regulatory/Procedural Matters to be Considered by the World Radiocommunication Conference 2019.* Accessed: Jan. 19, 2020. [Online]. Available: https://www.itu.int/dms_pub/itu-r/opb/act/R-ACT-CPM-2019-PDF-E.pdf

[3] D. M. Pozar, *Microwave Engineering*, 3rd ed. Hoboken, NJ, USA: Wiley, 2005.

[4] H. Wheeler, ''Simple relations derived fom a phased-array antenna made of an infinite current sheet,'' *IEEE Trans. Antennas Propag.*, vol. 13, no. 4, pp. 506–514, Jul. 1965.

[5] B. Munk, R. Taylor, T. Durharn, W. Croswell, B. Pigon, R. Boozer, S. Brown, M. Jones, J. Pryor, S. Ortiz, J. Rawnick, K. Krebs, M. Vanstrum, G. Gothard, and D. Wiebelt, ''A low-profile broadband phased array antenna,'' in *Proc. IEEE Antennas Propag. Soc. Int. Symp. Digest. Held Conjunct, USNC/CNC/URSI North Amer. Radio Sci. Meeting*, vol. 2, Jun. 2003, pp. 448–451.

[6] H. Zhang, S. Yang, S.-W. Xiao, Y. Chen, S.-W. Qu, and J. Hu, ''Ultrawideband phased antenna arrays based on tightly coupled open folded dipoles,'' *IEEE Antennas Wireless Propag. Lett.*, vol. 18, no. 2, pp. 378–382, Feb. 2019.

[7] Y. Wang, L. Zhu, H. Wang, Y. Luo, and G. Yang, ''A compact, scanning tightly coupled dipole array with parasitic strips for next-generation wireless applications,'' *IEEE Antennas Wireless Propag. Lett.*, vol. 17, no. 4, pp. 534–537, Apr. 2018.

[8] S. Xiao, S. Yang, H. Zhang, H. Bao, Y. Chen, and S.-W. Qu, ''A low-profile wideband tightly coupled dipole array with reduced scattering using polarization conversion metamaterial,'' *IEEE Trans. Antennas Propag.*, vol. 67, no. 8, pp. 5353–5361, Aug. 2019.

[9] R.-L. Xia, S.-W. Qu, S. Yang, and Y. Chen, ''Wideband wide-scanning phased array with connected backed cavities and parasitic striplines,'' *IEEE Trans. Antennas Propag.*, vol. 66, no. 4, pp. 1767–1775, Apr. 2018.

[10] J. A. Kasemodel, C.-C. Chen, and J. L. Volakis, ''Wideband planar array with integrated feed and matching network for wide-angle scanning,'' *IEEE Trans. Antennas Propag.*, vol. 61, no. 9, pp. 4528–4537, Sep. 2013.

[11] W. Zhou, Y. Chen, and S. Yang, ''Dual-polarized tightly coupled dipole array for UHF–X-band satellite applications,'' *IEEE Antennas Wireless Propag. Lett.*, vol. 18, no. 3, pp. 467–471, Mar. 2019.

[12] S. Ezhil Valavan, D. Tran, A. G. Yarovoy, and A. G. Roederer, ''Dual-band wide-angle scanning planar phased array in X/Ku-bands,'' *IEEE Trans. Antennas Propag.*, vol. 62, no. 5, pp. 2514–2521, May 2014.

[13] J. T. Logan, R. W. Kindt, M. Y. Lee, and M. N. Vouvakis, ''A new class of planar ultrawideband modular antenna arrays with improved bandwidth,'' *IEEE Trans. Antennas Propag.*, vol. 66, no. 2, pp. 692–701, Feb. 2018.

[14] M. H. Novak, F. A. Miranda, and J. L. Volakis, ''Ultra-wideband phased array for millimeter-wave ISM and 5G bands, realized in PCB,'' *IEEE Trans. Antennas Propag.*, vol. 66, no. 12, pp. 6930–6938, Dec. 2018.

[15] A. D. Johnson, S. B. Venkatakrishnan, E. A. Alwan, and J. L. Volakis, ''Suppressing E-plane scan resonance for UWB millimeter-wave differential phased array,'' in *Proc. Int. Appl. Comput. Electromag. Soc. Symp. (ACES)*, Apr. 2019, pp. 1–2.

[16] H. L. Zhu, S. W. Cheung, K. L. Chung, and T. I. Yuk, ''Linear-to-circular polarization conversion using metasurface,'' *IEEE Trans. Antennas Propag.*, vol. 61, no. 9, pp. 4615–4623, Sep. 2013.

[17] T. R. Cameron and G. V. Eleftheriades, ''Analysis and characterization of a wide-angle impedance matching metasurface for dipole phased arrays,'' *IEEE Trans. Antennas Propag.*, vol. 63, no. 9, pp. 3928–3938, Sep. 2015.

[18] S. Hussain and S.-W. Qu, ''A compact wideband, wide-scan millimeter-wave antenna array for 5G wireless applications,'' in *Proc. ICC-IEEE Int. Conf. Commun. (ICC)*, May 2019, pp. 1–5.

[19] D. M. Pozar, ''The active element pattern,'' *IEEE Trans. Antennas Propag.*, vol. 42, no. 8, pp. 1176–1178, Aug. 1994.

[20] S. M. Moghaddam, J. Yang, and A. A. Glazunov, ''A planar dual-polarized ultra-wideband millimeter-wave array antenna,'' in *Proc. 12th Eur. Conf. Antennas Propag. (EuCAP)*, Apr. 2018, pp. 1–3.

[21] M. H. Novak, J. L. Volakis, and F. A. Miranda, ''Low cost ultra-wideband millimeter-wave array,'' in *Proc. IEEE Int. Symp. Antennas Propag. (APSURSI)*, Jun. 2016, pp. 1841–1842.

SAJJAD HUSSAIN (Student Member, IEEE) was born in Khushab, Punjab, Pakistan. He received the B.Eng. degree in electrical engineering from Air University, Islamabad, Pakistan, in 2008, and the M.Sc. degree in telecommunication engineering from the University of Engineering and Technology (UET), Taxila, Pakistan, in 2013. He is currently pursuing the Ph.D. degree in electronics engineering (electromagnetic and microwave technology) with the University of Electronic Science and Technology of China (UESTC), Chengdu, China. His current research interests include UWB antennas and phased array antennas.
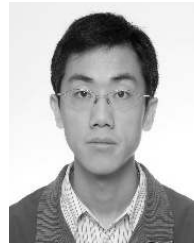
SHI-WEI QU (Senior Member, IEEE) was born in China, in 1980. He received the B.Eng. and M.Sc. degrees from the University of Electronic Science and Technology of China (UESTC), Chengdu, China, in 2001 and 2006, respectively, and the Ph.D. degree from the City University of Hong Kong (CityU), Hong Kong, in 2009. He was with the Tenth Institute of Chinese Information Industry, Taiwan, from 2001 to 2002. He was a Research Assistant with the Department of Electronic Engineering, CityU, from 2006 to 2007. He was a COE (Global Center of Excellence) Research Fellow and a Postdoctoral Fellow with Tohoku University, Sendai, Japan, from 2009 to 2010. He is currently an External Member of the State Key Laboratory of Millimeter Waves, Partner Laboratory, CityU, and also a Full Professor with the School of Electronic Engineering, UESTC. He has authored or coauthored over 70 internationally refereed articles and over 50 international conference papers. His current research interests include UWB antennas and arrays, phased arrays, and millimeter-wave/terahertz antennas and arrays.

WEN-LIANG ZHOU was born in Jiangxi, China, in 1994. He received the B.E. degree from the University of Electronic Science and Technology of China, Chengdu, China, in 2017, where he is currently pursuing the Ph.D. degree in electromagnetic and microwave technology. His current research interests include ultrawideband, wide angle scanning phased array antennas, and shared aperture antennas.

PENG ZHANG was born in Henan, China, in 1996. He received the B.Eng. degree in electronic engineering from the University of Electronic Science and Technology of China (UESTC), Chengdu, China, in 2018, where he is currently pursuing the M.Sc. degree in electromagnetic and microwave technology. His current research interests include dual-polarized antennas and phased arrays.

SHIWEN YANG (Fellow, IEEE) was born in Langzhong, Sichuan, China, in 1967. He received the B.S. degree in electronic science and technology from East China Normal University, Shanghai, China, in 1989, and the M.S. degree in electromagnetic and microwave technology and the Ph.D. degree in physical electronics from the University of Electronic Science and Technology of China (UESTC), Chengdu, China, in 1992 and 1998, respectively. From 1994 to 1998, he was a Lecturer with the Institute of High Energy Electronics, UESTC. From 1998 to 2001, he was a Research Fellow with the School of Electrical and Electronic Engineering, Nanyang Technological University, Singapore.

From 2002 to 2005, he was a Research Scientist with Temasek Laboratories, National University of Singapore, Singapore. Since 2005, he has been a Full Professor with the School of Electronic Engineering, UESTC. He has been a Chang-Jiang Professor nominated by the Ministry of Education of China, since 2015. He has authored or coauthored over 300 technical articles. His current research interests include antennas, antennas arrays, optimization techniques, and computational electromagnetics.

Prof. Yang was a recipient of the Foundation for China Distinguished Young Investigator presented by the National Natural Science Foundation of China, in 2011. He is currently the Chair of the IEEE Chengdu AP/EMC Joint Chapter and serves as an Editorial Board Member for the *International Journal of Antennas and Propagation* and the *Chinese Journal of Electronics*.

● ● ●